

MICROCAVITÉS ET CRISTAUX PHOTONIQUES *MICROCAVITIES AND PHOTONIC CRYSTALS*

Two-dimensional photonic crystals: new feasible confined optical systems

Henri Benisty, Maxime Rattier, Ségolène Olivier

Laboratoire de physique de la matière condensée, UMR 7643 du CNRS, École polytechnique,
91128 Palaiseau cedex, France

Received and accepted 23 November 2001

Note presented by Guy Laval.

Abstract

After a brief review of the basic properties of ideal two-dimensional photonic crystals, we describe the recent advances that have led to them being considered candidates in realistic, feasible optoelectronic systems that take advantage of their powerful light control capability. Two main fields of applications are integrated optics and microstructured fibres. We focus on the former one, closer to the genuine photonic gap concept. We illustrate through a number of optical elements – simple crystals, guides and cavities – the peculiarities of confinement by such systems. To cite this article: H. Benisty et al., C. R. Physique 3 (2002) 89–102. © 2002 Académie des sciences/Éditions scientifiques et médicales Elsevier SAS

photonic crystal / photonic bandgap / integrated optics / optical fibre / guide / cavity

Cristaux photoniques bi-dimensionnels : des systèmes optiques confinés nouveaux et faisables

Résumé

Après un bref passage en revue des propriétés de base des cristaux photoniques bi-dimensionnels idéaux, nous décrivons les avancées récentes qui montrent comment mettre à profit leurs puissantes capacités de contrôle de la lumière dans des systèmes optoélectroniques faisables. Deux des domaines d'application principaux sont l'optique intégrée et les fibres microstructurées. Nous nous concentrons sur le premier, plus proche du concept d'origine de bande interdite photonique. Nous illustrons au travers de divers éléments optiques – simple cristaux, guides, cavités – les particularités du confinement dans ces systèmes. Pour citer cet article : H. Benisty et al., C. R. Physique 3 (2002) 89–102. © 2002 Académie des sciences/Éditions scientifiques et médicales Elsevier SAS

cristal photonique / bande interdite photonique / optique intégrée / fibre optique / guide / cavité

1. Reminder on optical waveguides and confinement in optoelectronics

We shall mainly treat in this contribution photonic crystals implemented in a guided optics configuration, which typically consist of perforated circular holes traversing a monomode waveguide. We shall first recall

E-mail address: hb@pmc.polytechnique.fr (H. Benisty).

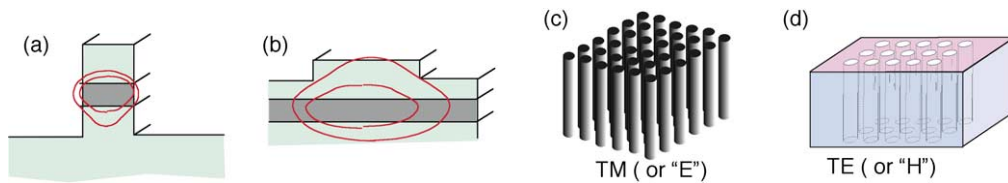


Figure 1. Basic concepts combined in this short review: (a) guided mode in a deep ridge waveguide, obtained by etching; (b) more loosely confined mode in a channel waveguide formed by a shallow ‘dielectric load’ obtained by lithography from an ordinary dielectric slab waveguide with subsequent etching or deposition; (c) 2D photonic crystal of the ‘dielectric pillar’ type, exhibiting preferentially a TM polarised gap (vertical electric field); (d) 2D photonic crystal of the hole-array-in-a-matrix type, having preferentially a TE polarised gap (vertical magnetic field).

briefly the various regimes of guiding in integrated optics in order to better place in context the peculiarities of photonic crystals.

Confinement in the field of optics is currently achieved in waveguiding systems, which are ubiquitous in, e.g., semiconductor heterostructures, glass fibres, etc. [1]. Planar slabs with a high-index layer sandwiched between lower index cladding layers have well-known guiding properties, with two well-defined TE and TM polarisations, allowing one to use a scalar field to describe these properties. To guide light along curved lines, if not using fibres, one may add an in-plane structuration to the above planar system that will confine light in one extra dimension. These structure typically come into two ‘flavours’ (Figs. 1a and 1b):

- (i) deep-etched ridge waveguides, where the lateral cladding is essentially air, and is thus very ‘strong’, and
- (ii) shallow-etched systems, or dielectric loaded guides, in which the thickness of the top cladding is locally larger, pinning an extra mode, with, however, a weaker barrier with respect to sideways optical leakage, as can be measured by the difference in propagation constant β of a mode of the slab and a mode of the etched guide, or, more commonly for practitioners in the field, the difference in effective index, $n_{\text{eff}} = \beta c / \omega$ (with the usual meaning of c and ω).

These channel guides require a full vector treatment in principle, but for many limit cases, one is sufficiently close to one of the parent slab guide polarisations to use it as a satisfactory basis. In both kinds of guiding, however, confinement has some limits. When it comes to bending channel guides, for example, solution (ii) is particularly poor and imposes a large radius of curvature, 1 cm in silica-based channel guides. The situation is better for solution (i) but still far from perfect: a sharp bend will lead to, e.g., mode coupling between quasi-TE and quasi-TM modes.

If one wants further confinement, for example, to define a lasing cavity, or a frequency-selective element, no compact solution is known to implement a mirror at a given position on a channel guide. The ubiquitous DBR solution (distributed Bragg reflector) [1–3] makes use of a shallow grating implemented usually by etching a sinusoidal grating in the cladding layer, leading to a very weak index perturbation; one thousand grating grooves are then needed to reach acceptable reflection, and only in the restricted spectral stop band of the DBR, less than 1% in relative extent $\Delta\lambda/\lambda$. These are some of the unsatisfactory facts in optoelectronics. Most attempts to etch stronger and more efficient gratings were plagued by very large radiation losses out of the guide that occur unless one obeys some geometric requirements on modulation depth that we will emphasise below and which are, in essence, those of two-dimensional photonic crystals etched through waveguides. Note however that even compact mirrors based on one-dimensional periodicity cannot provide omnidirectional confinement. In one-dimensional systems, the phase conditions which ensure a gap around a given angle of incidence cannot be maintained for all angles. There will unavoidably be a range of angles at which radiative modes exist through the periodic structure, so that it is impossible to build a perfect tiny ‘photon box’ based on such mirrors. The localised modes of such a box are broad in k -space and are thus liable to leak through the radiative modes.

One motivation towards the use of PCs and related localised photon structures is thus compact integration and diminished sizes, so that the 1000×1000 fibres optical switchboard of optical telecommunication systems remains small enough. This size reduction is also required in order to enable integration of more demanding functions such as wavelength transpositions at the nodes of a wavelength-multiplexed (WDM) network. Moreover, photonic crystals made of dielectrics can be very low-loss systems in the optical regime. Thus, they could replace metals in some cases as ‘optical insulators’.

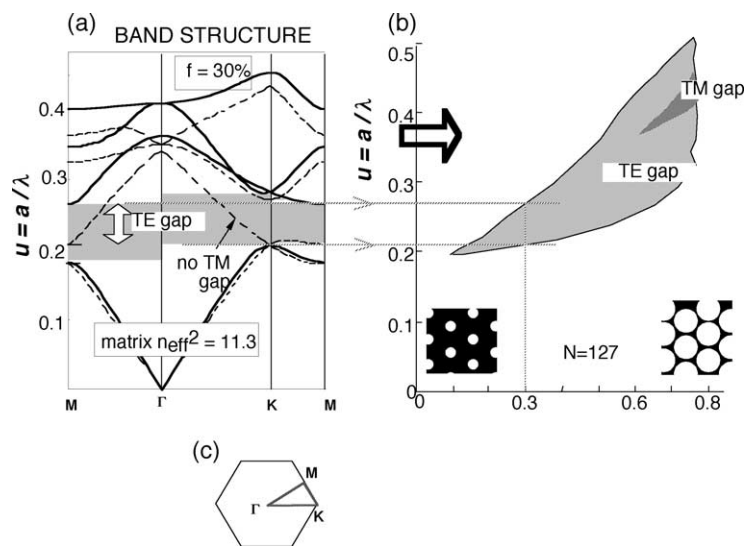
2. Basic properties of ideal two-dimensional photonic crystals

Following the three-dimensional PC concept proposed by Yablonovitch in 1987 [4], it was realised in the following years that periodic two-dimensional dielectric structures (with invariance along a third direction z) can also exhibit a photonic band gap [5,6], i.e., a range of frequency for which *in-plane* propagation is forbidden because there is no allowed propagative photon state, only evanescent ones. Photon states in periodic structures are described by a wavevector \mathbf{k} running in the Brillouin zone. As for the naming of polarisation, one uses E and H in pure 2D structures to denote those modes with the corresponding field along the invariant direction, the two components of the other field being in the periodicity plane. However, for the sake of consistency with guided optics approaches, we denote E as TM and H as TE.

Two kinds of dielectric structures easily provide a band gap at the first gap, as shown in Figs. 1c and 1d (the first gap is the one associated with about the half-wavelength periodicity, taking into account the material’s indices, however): the array of pillars provides a TM gap (Fig. 1c), while the array of holes (Fig. 1d) provide a TE gap. Then, since the central frequency of a gap at the edge of the Brillouin zone scales like the modulus of k , the preferred zone shape is as round as possible, which points to a hexagonal shape and thus a triangular lattice (of period denoted a). We concentrate here on the case of circular air holes (air rods) in a dielectric matrix, which has the advantage of much better compatibility with a dielectric waveguide implementation in the third direction. Let us introduce the air-filling factor f , which describes the areal amount of air in the 2D cross section of the PC.

An example of band structure $\omega(\mathbf{k})$ with a TE gap and no TM gap is given in Fig. 2a, for a system with dielectric constant $\epsilon_m = 11.3$ for the matrix and air-filling factor $f = 30\%$. The gap map of Fig. 2b represents the evolution of both TE and TM gaps in normalised frequency units of $u = a/\lambda = \omega a/2\pi c$ as a function of f . The Brillouin zone is sketched in Fig. 2c.

Figure 2. 2D photonic crystal consisting of a triangular lattice of cylindrical holes: (a) band structure $\omega(\mathbf{k})$ for a 30% air-filling factor. Note the overlap of the gap in the various directions; (b) ‘gap map’ describing the full gap evolution as a function of the air-filling factor f . Note the appearance of the TM gap on the right. Insets are typical low- and high- f lattices; (c) first Brillouin zone with the Γ , M and K points.



While the TE gap in a high-index material is obtained for rather low f values, $f = 10\text{--}15\%$, it turns out that a gap for both polarisations can be obtained at large f values, typically above $f = 65\%$, when veins between holes are thin and the shape left between three holes tends to be pillar-like. However, in the pure two-dimensional problem, hexagonal lattices of pillars may have quite similar properties to lattice of holes.

Semiconductors possess high enough refractive indices to fulfil the criterion of allowing a band gap common to both polarisation ($n > 2.6$), the criterion for a single polarisation being much less severe ($n \sim 2$ is enough in TE).

What are the basic reflection/transmission properties expected from an ideal two-dimensional PC [7,8]? Many cases are to be distinguished. For a beam impinging normal to the rod axis on a PC of, say, ten unit cells, one expects very weak transmission in the gap, of the order of 10^{-3} to 10^{-6} . Light not transmitted can be reflected, but also backward diffracted. In the case of air holes, the impinging medium has a high index (unperforated dielectric), and diffraction of the periodic surface of the PC is likely to occur in the first gap, typically with ± 1 diffracted orders allowed. A PC in the gap is thus both a grating and a mirror. Outside the gap, transmission is not granted [8,9]: it depends on the availability of a PC mode to fit the symmetry of the incoming wave, to ensure nonzero coupling. Hence, some ‘transmission gaps’ may occur while photonic states are present, these states being eventually able to carry away spontaneous emission from an atom situated inside the PC. Furthermore, when coupling is allowed, spectral transmission properties outside the gap are about those of ‘thick gratings’ [10], with spectral oscillations that depend on the phase taken by the excited Bloch wave upon achieving round trips in the PC sample. Below the first gap, at large wavelengths, a 2D PC behaves like a sub-wavelength structured material and displays a strong birefringence directly associated with the hole direction. The PC sample then behaves as a phase plate.

Finally, what happens at oblique incidence (with a k component along the invariance axis) [11]? The gap progressively shifts to higher frequency (basically, the same k component in the plane of periodicity is required) and vanishes for a few tens of degrees. The limit case of propagation along the invariance direction will be discussed specifically in relation with microstructured optical fibres. Let us only underline here that only the weaker transverse k components of the field (the ‘beam shape’) are then affected by the periodicity, and rather little remains from the original interference phenomenon, so that the concept of gap, and the conditions on index and periodicity are to be completely revised.

The only system to date in which structures close to ideal 2D PC have been fabricated in the near infrared is macroporous silicon, due to the extraordinary aspect ratio and shape perfection that is obtained by carefully implementing a photoelectrochemical etching method. Full 2D gaps in the $1.55\ \mu\text{m}$ region, hence with a period of about $600\ \text{nm}$, have been beautifully demonstrated recently [12–17].

3. Defect states

One can classify defects in 2D PC according to their dimensionality: ‘0D’ defects are formed by missing rods or just one or a few modified holes. Such defects introduce modes with eigenfrequencies in the gap. Even a single missing hole supports several such modes within the gap. The photon-in-a-box mode-counting tells us that the number of states in the gap scales like the defect area S . For, e.g., the $f = 30\%$ crystal described above, one finds about 0.3 state per missing hole and per 10% bandwidth (about the gap relative width).

Another canonical class of defects are line defects formed along dense rows according to the schemes of Fig. 3, a–b, whereby a spacer of thickness L_c is introduced. The two halves are PC-based mirrors so that, at normal incidence, it is basically a Fabry–Perot (FP) cavity [18,19] at $k_{\parallel} = 0$; owing to the periodicity, the modes may be classified using k_{\parallel} [20]. For infinitely thick mirrors, there is no fundamental distinction between the $k_{\parallel} = 0$ FP modes and modes with k_{\parallel} as high as allowed, in the sense that energy remains confined in the cavity for any frequency in the gap. For mirrors of finite PC thickness, say a few rows, the modes unavoidably experience a finite coupling to outside radiations, allowing, e.g., unit transmission at resonance for a symmetric configuration. This system is also a waveguide that will convey energy or

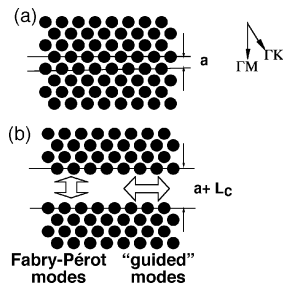


Figure 3. (a) Piece of eight rows of 2D PC with ΓM and ΓK directions; (b) a separation of dimension L_c is introduced between the upper and lower four rows. This spacer allows the formation of Fabry-Pérot type modes in the gap, as well as ‘guided’ modes. Note that no clear distinction can be made in the absence of a genuine critical angle here.

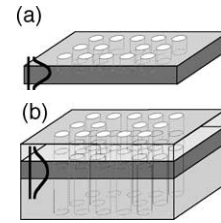


Figure 4. PC in a slab waveguide: (a) membrane limit, obtained in practice by the selective dissolution of a sacrificial layer beneath the membrane; (b) case of a conventional heterostructure waveguide, with modest index steps between the core and cladding. In this case, the holes also have to be drilled down in the bottom cladding as much as possible.

signal efficiently if the modal group velocity $d\omega/dk_{\parallel}$ is sufficiently high (for the FP mode, it is zero!). This is closely related to the issue of integrated optics telecommunication systems, and to the possibility of bending, combining, splitting such waveguides. This will be examined in more detail below. We now turn to the experimental systems, for which the third dimension is quantised.

4. Photonic crystals etched through a waveguide

4.1. PCs in membrane systems

The superb achievement of macroporous-silicon PCs cannot, unfortunately, be transposed to other materials, except alumina. Then, as far as finite height structures are concerned, it makes sense to freeze the third (vertical) degree of freedom by etching holes in a dielectric waveguiding structure. Self-supported membranes are the thinnest such structures (Fig. 4a), and are thus relatively easy to etch. One dissolves a sacrificial layer beneath the membrane by selective etching, a process best mastered in InP-based alloys [21,22], and also available for silicon-on-silica through selective, hydrofluoric-acid-based etching of the latter material [23,24]. A virgin membrane always sustains at least one guided mode. But given the high index contrast, the minimum guided mode extent corresponds to a membrane thickness of the order of $\lambda/2n$, hence $0.2 \mu\text{m}$ for near-infrared applications.

If the system is infinite, modes are again properly labelled by k_{\parallel} , the in-plane wavevector, restricted to the first Brillouin zone. Radiation modes have a real k_z component in the third direction so that $\omega = c\sqrt{k_{\parallel}^2 + k_z^2} > ck_{\parallel}$. If a mode lies below the vacuum light line $\omega = ck_{\parallel}$ of the dispersion diagram (Fig. 5), it cannot couple to radiation modes for which $\omega > ck_{\parallel}$ (all higher Fourier components, outside the first Brillouin zone, feature larger k and automatically obey $\omega < ck$). Upper dispersion branches lying in the region $\omega > ck_{\parallel}$ correspond to modes filling in principle the full space, but for which sizeable localisation in the membrane is still possible. The other way round, one can view these modes as guided modes with a relatively well-defined k_{\parallel} value and a modest coupling to the outside. Such resonant modes give rise to anomalies in transmission or reflection of impinging plane waves at a characteristic angle, a phenomenon known in lamellar gratings (related to the surface plasmon of the coating metal, indeed), and which can be traced back to the Wood anomaly of metallic gratings (see [25,26] for the case of PCs). Close but distinct from the 2D-PC geometry is the air-bridge geometry probed by Villeneuve et al. [27], with 1D rather than 2D periodicity and few periods. In these studies, however, the emphasis has been more on gaps and defect modes than on dispersion relations and existence of true guided modes.

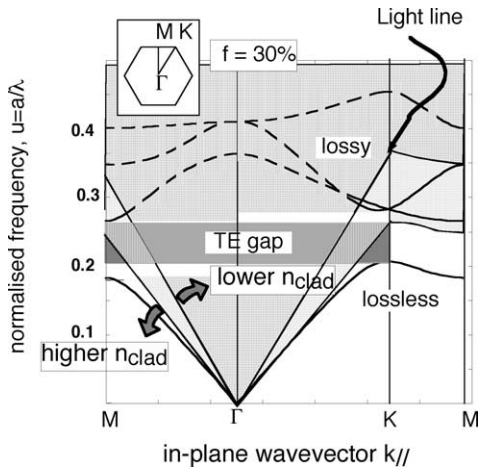


Figure 5. Previously shown bandstructure with the superimposed light lines for two cladding indices. A vanishing area of the useful TE gap remains below such light lines, if at all.

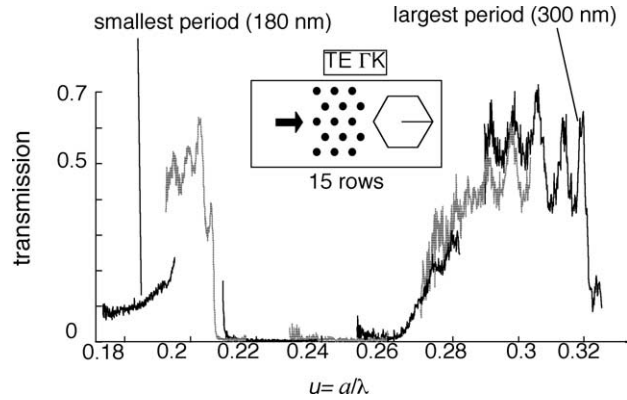


Figure 6. Transmission spectrum along the ΓK axis and for the TE polarisation of 15 rows of 2D PC, with about 21% filling factor. The support is a laser-like Ga(Al)As based waveguide. Such a spectrum is actually glued from spectra obtained with different periods a , plotted as a function of the normalised frequency $u = a/\lambda$. Note the gap from $u = 0.21$ to $u = 0.27$, and its steep low-frequency edge. Probing light stems from the photoluminescence of InAs dots embedded in the GaAs core.

Experiments on membrane-based PCs have been first devoted to 0D defects such as micro-hexagons, with a continued string of results [21,28–32]. Recently, emphasis has turned towards waveguiding in, e.g., single missing row waveguides [24,33,34], and back to PCs themselves in the Tsukuba group [35]. Coming back to the 0D defect, the associated localised mode has a continuous k -spectrum, giving rise to k -components *above* the light line (i.e., closer to $k = 0$ at given ω). Electromagnetic energy of such a defect mode eventually radiates into 3D modes [36,37]. This unavoidable channel establishes an upper limit to the damping rate of energy trapped in the defect state.

In terms of light-emitting device, this channel indeed corresponds to a perfect extraction efficiency, whereby light generated inside a dielectric is fully radiated outside [38,39]. This resolves in principle one of the recognised difficulties towards high-efficiency light sources based on high index materials, a goal actively pursued in the fast growing area of high-brightness LEDs [40], in view of the huge lighting market. However, a membrane system does not qualify as a mass-production device [38,39].

Self-supported membranes are thus probably excellent laboratory systems but one may prefer more robust ones. An easy way to strengthen such membranes is to bond them to a glass substrate ($n_s \approx 1.46$) and lift them off their original substrate [33]. This has the clear drawback of lowering the light line down to $\omega = ck_{\parallel}/n_s$, meaning that at a given ω , higher k_{\parallel} are able to radiate into substrate modes and damp possible defect modes. A route more adapted to GaAs-based heterostructures is to selectively steam-oxidise a high Al-content GaAlAs layer into ‘AlOx’, of index $n_s \approx 1.6$ [41].

The AlOx system has been used for air bridges [27], and recently for 2D PCs [42], with moderate success in terms of optical performances, with the exception of a recent breakthrough for a bent waveguide [43].

4.2. PCs in conventional guiding systems

What happens with a more classical guiding heterostructure with moderate index contrast, ($\Delta n = 0.2$ to 0.6, Fig. 4b)? The penalty is to lower the light line down to $\omega = (c/n_{\text{clad}})k_{\parallel}$ so that all the 2D photonic gap is unfortunately above the light line and to subsequently allow many more k components of a given mode

to radiate away from the guide. We will discuss below conditions for out-of-plane radiation losses to be nevertheless acceptable. Following the work by Krauss [44], a collaboration associating our laboratory, the University of Glasgow (C. Smith and T.F. Krauss) and École Polytechnique Fédérale de Lausanne (EPFL, R. Houdré, R. Stanley, U. Oesterle, M. Ilegems) has acquired extensive experience of this kind of 2D PCs for filling factors f in the range 20–40%, where out-of-plane radiation losses are still affordable.

A quite complete set of transmission, reflection and diffraction measurements of 2D PCs of this kind, etched through a GaAs-based laser-like heterostructure, using photoluminescence of quantum wells or InAs quantum dots as an internal and very practical light source, can be found in the following references [31,45–48]. With QDs, this source is relatively broadband ($> 10\%$), so that combined with ‘lithographic tuning’ with $\sim 10\%$ steps of the PC period a , a continuous spectrum is obtained. Typical periods to obtain a gap around $1 \mu\text{m}$ are $a = 200\text{--}240 \text{ nm}$, and nominal hole diameters 130 to 160 nm.

Such a combined spectrum using variable periods a (from 180 to 330 nm) is presented in Fig. 6 for $N = 15$ rows along the ΓK orientation. The full gap (overlap with the ΓM gap) extends from $u = 0.21$ to $u = 0.245$, over a 15% relative frequency range. Oscillations around the gap are clearly visible. As discussed in [31,46] these oscillations are associated with the interference of Bloch waves undergoing Fabry–Perot type round-trips across the whole crystal (15 rows). Hence, the sizeable amplitude of these oscillations demonstrates that a Bloch wave launched at one crystal side suffers modest attenuation upon a round-trip through 30 rows of cylinders, about 60 semiconductor/air interfaces. The good accuracy of the pure 2D picture to depict this system indicates that the various perturbations (fabrication fluctuations and mostly radiation losses) are still modest.

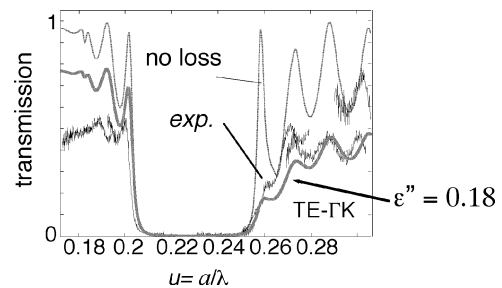
The present authors also belong to a European IST consortium ‘PCIC’, IST 11239, gathering teams from Wurzburg University, EPFL (Lausanne), Opto+ in Marcoussis (France), KTH in Kista (Sweden), LPN in Marcoussis (France) and FORTH (Heraklion). This consortium has recently achieved PCs with about similar spectral behaviour in an InP-based heterostructure, using a single QW as a $\sim 1.5 \mu\text{m}$ internal light source, and closely spaced periods to compensate for the insufficient useful spectral width of the source (about 50 nm) [49]. This validates the generality of the concept, and shows that provided adequate etching is available, PCs exhibit the expected properties.

4.3. The issue of out-of-plane radiation loss

Recent progress has taken place in evaluating out-of-plane radiation losses of ‘conventional’ heterostructures; this shall be reviewed first. In Fig. 6, the damping of the oscillation amplitude on the high energy side of the gap reveals large losses when the Bloch wave samples the holes rather than the dielectric. This confirms the intuition that losses occur in the air holes due to the absence of waveguiding. A more quantitative perturbation scheme was set up in reference [50] based on separability considerations. The radiation losses then appear to stem from the radiation of effective dipoles that are proportional to the (average) field E_h in the hole, the hole area itself and to the vertical dielectric contrast of the heterostructure, denoted $\Delta\epsilon$ [50]. Radiation losses, essentially the square of the dipole’s emitted power, are thus proportional to $E_h^2(\Delta\epsilon)^2$. One can then view them in a two-dimensional approach as a dissipative loss by attributing to the air holes

Figure 7. Comparison of the experimental results of Fig. 6 with a perfect, purely 2D, lossless model (dotted line) that would correspond to the structure of Fig. 1d.

The dashed line is for a similar system with an imaginary part of the dielectric constant $\epsilon^* = 1 + 0.18i$ added in the holes: the dissipation occurring in this waveguide-less system then accounts well for the radiation losses actually occurring in the waveguide geometry.



an ad hoc imaginary constant ε'' . Fig. 7 show the success of a fit of the transmission data of Fig. 6 above, made with $\varepsilon'' = 0.18$ in a simple 2D model [50]. The ability to cast losses of a complex 3D structure into a single number is indeed quite valuable and may help selecting among various approaches otherwise delicate to compare.

Since then, Lalanne [51] has proposed an exact three-dimensional calculation of the above systems which has led to the following refinement: the value of losses pointed out in [50] stems at 80–90% from the finite hole depth z_0 , a depth which obviously depends on the PC period due to well-known properties of the etching procedure. From this point on, we have established [52] that the excess radiation losses due to finite hole depth scale essentially like the partial confinement factor $\Gamma(z_0)$ of the guided wave profile with the unetched part of the hole. This is the key to quantifying the issue “How deep do I have to etch?”; the other side of this issue is “how much are the intrinsic losses” associated with infinite hole depth. Lalanne’s calculation points to a level of $\varepsilon'' \sim 0.2$ for the GaAs system and etching we have used until now, and for which the vertical contrast is still relatively large ($\Delta\varepsilon = 2$). Hence, going to low contrast systems such as InP ($\Delta\varepsilon = 0.5$), and achieving sufficient etch depth ($\Gamma(z_0) < 10^{-3}$) would probably result in a loss parameter $\varepsilon'' \sim 0.005$, which would bring these systems very close to ideal ones, with loss-limited reflectivities in the 99.5% range, not so far from those of the excellent vertical DBRs used in VCSELs.

As for out-of-plane losses of the membrane system, there is some consensus on the overall picture: in periodic systems, which include straight guides below, there is some common room between the photonic gap and the light line, so that lossless propagation of modes along a 1D defect is possible. But as soon as periodicity is broken, as happens for PC-based guide bends and cavities, radiation losses are again there, and it is likely that they are relatively strong: using our perturbation approach, membranes feature a very high $\Delta\varepsilon$ of about 10. The situation is thus complex, only that part of the field concerned with the device singularity radiates, no modelling tool appears to be able to cast this phenomenon in 2D and loss modelling has to be made on a time-consuming, per-device basis.

Another delicate issue in both systems is the coupling in and out of PC structures. While our ε'' ansatz seems to account satisfactorily for such losses in ‘conventional’ substrates, a recent study by Bogaerts et al. [53] suggests that high losses occur at transitions towards membrane type PCs.

5. Controlling light with PCs

5.1. Cavities

The two classes of cavity modes introduced above, ‘0D’ and ‘1D’ have also been experimentally demonstrated using the same waveguide-based GaAs-based and InP-based PCs. Micro-hexagons of a few a have been fabricated in either the membrane or the conventional systems and probed using the internal

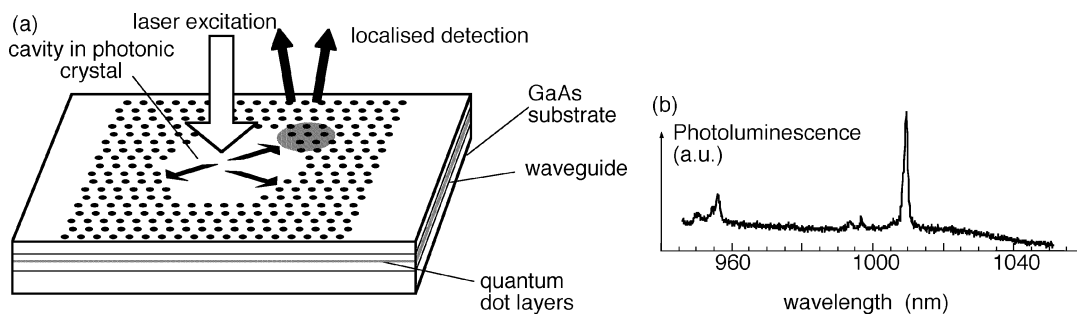


Figure 8. Probing resonators by means of internal excitation of internal emitters (e.g., InAs dots): (a) experimental scheme of laser excitation, in-plane resonator and localised light collection; (b) typical measured spectrum showing high- Q resonances ($Q \sim 1000$).

PL of embedded QWs or, better, QDs photoexcited inside the cavity (Fig. 8a) [21,28–32]. Various detection schemes have been used [29,54]. A typical spectrum for our conventional GaAs-based systems is shown in Fig. 8b for a cavity of side $5a$ (61 missing holes). Narrow peaks with $Q \sim 1000$ clearly appear, which are the signature of in-plane cavity modes. Note the relative scarcity of these peaks: one expects about 20 modes expected for the 10% present relative bandwidth and cavity size. This stems from the poor far-field pattern of most of the in-plane modes, which has no reason to give a single lobe towards the collecting optics, unless the mode is especially symmetrical. These sharp spectral peaks are, anyway, a wonderful fabrication reproducibility test [30,31].

To obtain, in the simplest way, quantitative information on the quality of confinement, we found that 1D defects (Fabry–Perot cavities bounded by PCs) were most interesting [18,19] and in particular, they allow easy insight into the mirror losses. For PCs of $N = 4$ rows only, and still the same kind of air-filling factors (20–40%), we introduced a spacer L_c of a few a .

While one expects unit transmission and quality factors of the order of 200–250 in the lossless limit, we found peaks with quality factors Q from 50 to 200 and peak transmissions from 15% to 45% [18,19]. Corresponding mirror reflectivities are about $R = 90\%$, with transmission T and losses L each 5% of the remaining 10% power ($T + R + L = 1$). This shows experimentally that conventional systems can compete well with membranes in terms of reflectivity. Until now, few unambiguous numbers have been published on the reflectivity of PCs in membranes [21,55].

5.2. Guides, bends and couplers

Studies on guides and related integrated optics elements (bends, couplers, splitters) started in 1999, with a qualitative contribution [33] and have flourished since then. Along the road of PCs in conventional systems, we have demonstrated low-loss guiding (losses less than 50 cm^{-1}), coupling of a cavity and a nearby guide [56], and recently, resonant transmission at a bend by means of an inserted cavity [57]. Studies on bends and combiners are also being carried out on InP and GaAs in the framework of PCIC [58,59], with the successful introduction of end-fire techniques to measure PC guides inserted between ridge guides.

In membrane systems, a number of groups have produced interesting results very recently, among which are references [43,60] for GaAs on AlOx, [35] for AlGaAs membranes, [24] for SOI, and [61] for a drop filter on InP. To make a long story short, let us say that, by far, no fully satisfying system has yet appeared, e.g., with broadband bending capability, monomode behaviour and low loss. Presently, no clear estimate of the definite merits of all these approaches can be made. In addition to the intrinsic optical figure of merit of any of them, one should also consider how easy it is to cascade elements, what kind of application is sought, and in particular whether active devices with PCs are sought [62].

One of the delicate application issues in both cases is to reach an accuracy compatible with the forthcoming wavelength division multiplexing (WDM) standards, either 100 GHz channel spacing with flat 40 GHz top, which translate into cavity Q of at least 5000, or 25 GHz spacing for denser systems, with Q around 20 000. These grids are agreed by the ITU (International Telecommunication Union) and are called the ITU grids. Not only are such high Q needed, but also, an array of tens or hundreds of such cavities aligned with this ITU grid is required. Presently, the only envisioned solution is post fabrication tuning, either mechanical or electro-optical. The area of mechanical-electrical-micro-systems (MEMS) devoted to optoelectronics (hence, MOEMS) could provide the desired tuning schemes.

6. Active devices

As PCs were originally devised to control spontaneous emission, it is interesting to include them in light-emitting devices, namely LEDs and lasers. The ultimate control with an emitter coupled to one or two optical defect modes is however extremely difficult in terms of practical applications because of the large nonradiative losses induced at etched interfaces, which translates into poor injection yields into the active quantum states whose optical environment is modified. In GaAs, only some cryogenic model systems

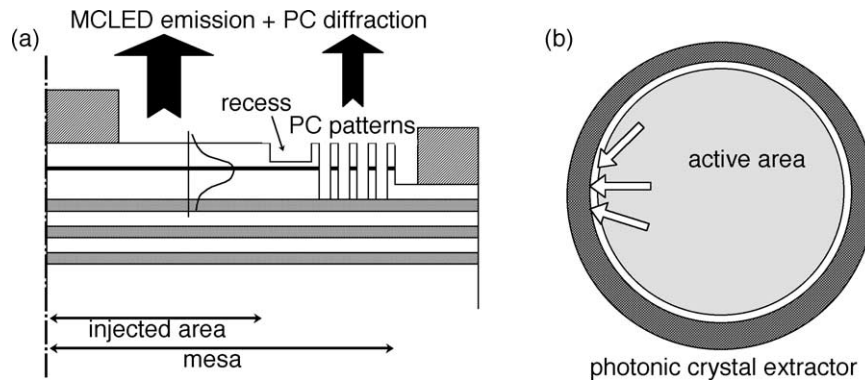


Figure 9. Use of photonic crystal for light extraction in a microcavity-LED: (a) side view, showing the microcavity formed between an air-GaAs interface and a few layers of Bragg mirrors, possibly insulating AlO_x-based Bragg mirrors. The guided mode carries away a large part of the power from the active layer, which is extracted at the periphery of the device; (b) top view, showing that the light in the guided mode impinges on the extracting structures under a wide range of angles.

(pillars, microdiscs) using quantum dots have shown such interactions. In InP, the much lower nonradiative recombination penalty has allowed the impressive achievement on a membrane of a room temperature optically injected laser based on a single missing hole and a very small (although not ultimate) associated mode [63,64].

A rather different approach is to seek the modifications of spontaneous emission, and in particular light extraction, in an infinite 2D PC. Of course, when it is of the slab type, and in-plane propagation is forbidden, very high extraction arises. The more realistic situation of partially etched waveguides has been addressed in some detail by Rigneault [65].

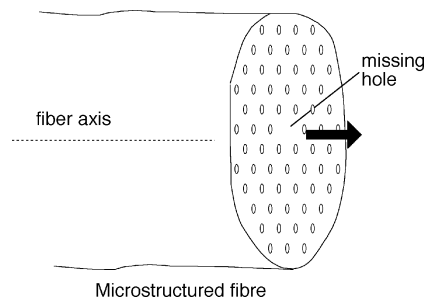
Scanning towards large sizes, we find the above mentioned laser realisation by Raffaele [62], which can readily be transformed into a 2D PC laser, the use of PCs as laser mirrors [66] or to make ‘bent lasers’ [67], and the work on extraction by Borodistky [39] which is more aimed at enhanced extraction for LEDs. We have pursued the use of PCs in somewhat larger LEDs, with the aim of using them as extractors of the guided mode at the periphery of the active emitting area [41]. The two-dimensional aspect allows light extraction for a nontrivial set of incidence angles onto the crystal (Fig. 9), a welcome property for extraction. The optical properties of these PCs are just the converse of what is expected in integrated optics: no reflection, high radiation losses, in relatively precise directions moreover.

There is however some room to revisit the numerous early day ideas with the concepts of integrated optics; some such ideas are coupled cavity lasers, power laser diodes and echelle grating integrated spectrometers [68] which were abandoned because of the poor properties (structural and optical) of etched interfaces. The advent of novel etching techniques together with the powerful design window opened by PCs is full of promises.

7. Microstructured fibres

Microstructured optical fibres (MOFs), although they belong to a rather different domain of applications and tend to address electromagnetism in a somewhat different way given the propagation along the invariant direction, still retain some of the magic of periodic objects. See [69] and references therein for updated state-of-the-art. Even though the glass/air index contrast is modest, a periodic or even simpler microstructure in a glass fibre may have a huge impact on its modal propagation properties. For a MOF with z axis, guided modes have a k_z component much larger than the transverse ones k_x, k_y . A forbidden band of a periodic microstructure is then no longer a frequency band with no propagative state at all for in-plane directions,

Figure 10. One of the typical layout of silica-based microstructured fibres, consisting of an array of holes, with a missing hole at the centre that anchors the mode. Another alternative is to guide light within an air core using the virtual absence of light leakage through a properly designed periodic air/silica structure.



but rather a band with no allowed k_x, k_y states given some value of k_z . If one creates a defect (the core of the MOF) in the middle of the periodic structure that can sustain a mode with the adequate k_z , it will be a bound mode. These MOFs are simple to fabricate from cm-width preforms that are manually stacked with, e.g., some missing ones. Two steps of elongation result in a preserved shape scaled down to the micron scale. Of course, MOFs in a general sense have existed for a long time, e.g., the ‘W’ fibre and polarisation maintaining ‘panda’ fibres, but the study of periodicity-based MOFs has been prompted by the PC concepts.

Two main kinds of new MOFs are focussing the highest interest:

- (i) ‘Eternally monomode fibres’ which retain this property over very large spectral ranges, e.g., from visible to 1550 nm. This is due to the ‘modal sieve’ property of the assembly of the triangular array of holes around the core (Fig. 10): any mode that has two lobes in the core is also allowed to extend into the PC part and loses its guided character. Then, at long wavelength, modes are broad and tend to see the average PC index, while at short wavelength, they are wavy enough to have nodes at the holes of the PC and see the higher glass index. The complicated transition between these regimes strongly affects dispersion. In particular, it allows the zero group velocity delay wavelength to be placed almost anywhere, e.g., around the standard VCSELs wavelengths of 850 nm, meaning that picosecond pulses may then travel undistorted for kilometres, avoiding the fate of near infrared pulses in conventional fibres.
- (ii) Fibres supporting a mode essentially in the air, with guidance from the 2D PC Bragg reflection (no total internal reflection from air!). This requires quite a lot of air also in the PC cladding. The interesting property here is to push away the thresholds for nonlinearities due to the much reduced glass–wave interaction. Nonlinearities are one of the main limits to fibre capacities. It is hoped that the launching of waves with powers of watts rather than 10 mW could take place at these fibre entrances without this penalty. The use of such ‘high power fibres’ in laser-machining with a remote, nonmoving laser is also envisioned.

We will not detail these two types further, but we just note that the losses and imperfections of these fibres, which limited early experiments in 1996–1998 to centimetric samples, are now much lowered, with preliminary reports of kilometre long operation for the more robust scheme (i) above (see CLEO 2001 post-deadline papers).

8. Conclusions

Optical confinement in more than one dimension has been for a long time a challenge: in optics, basic microstructures based on metals tend to be lossy, and are anyway not easy to fabricate; the concept of photonic crystal has fed many novel approaches. While it is at its best in theory in 3D, it is clear that deterministic structures are much more practical in 2D. Providing the third confinement by means of a conventional waveguide allows recovery of much of what is expected in 3D, e.g., the ability to produce high- Q photonic boxes. Most of what we have presented is of obvious interest for integrated optics, a field in which the planar waveguide is also the basis. PCs in two dimension provide efficient mirrors and cavities (of interest in novel laser devices), they certainly have a high potential to produce by a single lithographic

step a number of functions such as filtering, guiding, bending, etc., which are beyond the scope of such a short review, but for which realisations have progressed at an impressive pace during these last two years. For simpler devices such as individual high-brightness LEDs and lasers, these 2D PCs also offer new ways to tackle the electromagnetic issues that are at the heart of the attainment of high, ultimate performances for such devices.

Finally, due to their simplicity of use combined with rapid progress in fabrication, microstructured optical fibres that directly treat existing fibre signals from the point of view of dispersion, nonlinearity, etc., are expected to be among the first photonic-crystal related products on the market place, in addition to taking an increasing role as a model system in the (engineering) academic realm.

Acknowledgements. The authors acknowledge the support of the European ESPRIT project ‘SMILED’ and of the European IST project ‘PCIC’.

References

- [1] T. Tamir (Ed.), *Guided Wave Optoelectronics*, Springer-Verlag, Berlin, 1990.
- [2] C. Weisbuch, J. Rarity (Eds.), *Microcavities and Photonic Band Gaps: Physics and Applications*, Kluwer, Dordrecht, 1996.
- [3] H. Benisty, J.-M. Gérard, R. Houdré, J. Rarity, C. Weisbuch (Eds.), *Confined Photon Systems: Fundamentals and Applications*, Springer, Heidelberg, 1999.
- [4] E. Yablonovitch, Inhibited spontaneous emission in solid-state physics and electronics, *Phys. Rev. Lett.* 58 (1987) 2059–2062.
- [5] R.D. Meade, K.D. Brommer, A.M. Rappe, J.D. Joannopoulos, Existence of a photonic band gap in two dimensions, *Appl. Phys. Lett.* 61 (1992) 495.
- [6] J.D. Joannopoulos, R.D. Meade, J.N. Winn, *Photonic Crystals, Molding the Flow of Light*, Princeton University Press, Princeton, NJ, 1995.
- [7] M. Sigalas, C.M. Soukoulis, E.N. Economou, C.T. Chan, K.M. Ho, Photonic band gaps and defects in two dimensions: studies of the transmission coefficient, *Phys. Rev. B* 48 (1993) 14121–14126.
- [8] K. Sakoda, Symmetry, degeneracy, and uncoupled modes in two-dimensional photonic lattices, *Phys. Rev. B* 52 (1995) 7982.
- [9] W.M. Robertson, G. Arjavalingam, R.D. Meade, K.D. Brommer, A.M. Rappe, J.D. Joannopoulos, Measurement of photonic band structure in a two-dimensional periodic array, *Phys. Rev. Lett.* 68 (1992) 2023–2026.
- [10] H. Kogelnik, C.V. Shank, Coupled wave theory of distributed feedback lasers, *J. Appl. Phys.* 43 (1972) 2327–2335.
- [11] X.-P. Feng, Y. Arakawa, Off-plane dependence angle of photonic band gap in a two-dimensional photonic crystal, *IEEE J. Quantum Electron.* 32 (1996) 535–541.
- [12] U. Grüning, V. Lehmann, S. Ottow, K. Busch, Macroporous silicon with a complete 2D PBG centered at 5 μm , *Appl. Phys. Lett.* 68 (1996) 747–749.
- [13] S. Rowson, A. Chelnokov, J.-M. Lourtioz, Macroporous silicon photonic crystals at 1.55 micrometers, *Electron. Lett.* 35 (1999) 753–755.
- [14] A. Birner, U. Gruning, S. Ottow, A. Schneider, F. Müller, V. Lehmann, H. Föll, U. Gösele, Macroporous silicon: a two-dimensional photonic bandgap material suitable for the near-infrared spectral range, *Phys. Status Solidi A* 165 (1998) 111–117.
- [15] S. Rowson, A. Chelnokov, J.M. Lourtioz, F. Carcenac, Reflection and transmission characterisation of a hexagonal photonic crystal in the mid infrared, *J. Appl. Phys.* 83 (1998) 5061.
- [16] S.W. Leonard, H.M. van Driel, A. Birner, U. Gösele, P.R. Villeneuve, Single-mode transmission in two-dimensional macroporous silicon photonic crystal waveguides, *Opt. Lett.* 25 (2000) 1550–1552.
- [17] S.W. Leonard, H.M. van Driel, K. Busch, S. John, A. Birner, A.-P. Li, F. Müller, U. Gösele, V. Lehmann, Attenuation of optical transmission within the band gap of thin two-dimensional macroporous silicon photonic crystals, *Appl. Phys. Lett.* 75 (1999) 3063–3065.
- [18] C.J.M. Smith, T.F. Krauss, R.M. De La Rue, D. Labilloy, H. Benisty, C. Weisbuch, U. Oesterle, R. Houdré, In-plane microcavity resonators with two-dimensional photonic bandgap mirrors, *IEE-Proc.-Optoelectron.* 145 (1998) 373–378.
- [19] M. Rattier, H. Benisty, C.J.M. Smith, A. Béraud, D. Cassagne, T.F. Krauss, C. Weisbuch, Performance of waveguide-based two-dimensional photonic-crystal mirrors studied with Fabry–Pérot resonators, *IEEE J. Quantum Electron.* 37 (2001) 237–243.
- [20] H. Benisty, Modal analysis of optical guides with two-dimensional photonic band-gap boundaries, *J. Appl. Phys.* 79 (1996) 7483–7492.

- [21] P. Pottier, C. Seassal, X. Letartre, J.L. Leclercq, P. Viktorovitch, D. Cassagne, C. Jouanin, Triangular and hexagonal high Q-Factor 2D photonic bandgap cavities on III–V suspended membranes, *J. Lightwave Technol.* 17 (1999) 2058–2062.
- [22] N.L. Dantec, T. Benyattou, G. Guillot, A. Spisser, C. Seassal, J.L. Leclercq, P. Viktorovitch, D. Rondi, R. Blondeau, Tunable microcavity based on InP-Air Bragg mirrors, *IEEE J. Quantum Electron.* 5 (1999) 111–114.
- [23] M. Loncar, T. Doll, J. Vuckovic, A. Sherrer, Design and fabrication of silicon photonic crystal optical waveguides, *J. Lightwave Technol.* 18 (2000) 1402–1411.
- [24] M. Loncar, D. Nedeljkovic, T. Doll, J. Vuckovic, A. Sherrer, T. Pearsall, Waveguiding in planar photonic crystals, *Appl. Phys. Lett.* 77 (2000) 1937–1939.
- [25] V.N. Astratov, I.N. Culshaw, R.M. Stevenson, D.M. Whittaker, M.S. Skolnick, T.F. Krauss, R.M.D.L. Rue, Resonant coupling of near-infrared radiation to photonic band structure waveguides, *J. Lightwave Technol.* 17 (1999) 2050–2057.
- [26] D.M. Whittaker, I.S. Culshaw, Scattering-matrix treatment of patterned multilayer photonic structures, *Phys. Rev. B* 60 (1999) 2610–2618.
- [27] P.R. Villeneuve, S. Fan, J.D. Joannopoulos, K.Y. Lim, G.S. Petrich, L.A. Kolodzejski, R. Reif, Air bridge microcavities, *Appl. Phys. Lett.* 67 (1995) 167–169.
- [28] R.K. Lee, O.J. Painter, B. D’Urso, A. Scherer, A. Yariv, Measurement of spontaneous emission from a two-dimensional photonic band gap defined microcavity at near-infrared wavelengths, *Appl. Phys. Lett.* 71 (1999) 1522–1524.
- [29] C.J.M. Smith, T.F. Krauss, R.M. De La Rue, D. Labilloy, H. Benisty, C. Weisbuch, U. Oesterle, R. Houdré, Near-infrared microcavities confined by two-dimensional photonic bandgap crystals, *Electron. Lett.* 35 (1999) 228–230.
- [30] C.J.M. Smith, T.F. Krauss, H. Benisty, M. Rattier, C. Weisbuch, U. Oesterle, R. Houdré, Directionally dependent confinement in photonic-crystal microcavities, *J. Opt. Soc. Am. B* 17 (2000) 2043–2051.
- [31] H. Benisty et al., Optical and confinement properties of two-dimensional photonic crystals, *J. Lightwave Technol.* 17 (1999) 2063–2077.
- [32] C. Reese, C. Becher, A. Imamoglu, E. Hu, B.D. Gerardot, P.M. Petroff, Photonic crystal microcavities with self-assembled InAs quantum dots as active emitters, *Appl. Phys. Lett.* 78 (2001) 2279–2281.
- [33] T. Baba, N. Fukaya, J. Yonekura, Observation of light propagation in photonic crystal optical waveguides with bends, *Electron. Lett.* 35 (1999) 654–655.
- [34] M. Tokushima, H. Kosaka, A. Tomita, H. Yamada, Lightwave propagation through a 120° sharply bent single-line-defect photonic crystal waveguide, *Appl. Phys. Lett.* 76 (2000) 952–954.
- [35] N. Kawai, K. Inoue, N. Carlsson, N. Ikeda, Y. Sugimoto, K. Asakawa, T. Takemori, Confined band gap in an air-bridge type of two-dimensional AlGaAs photonic crystal, *Phys. Rev. Lett.* 86 (2001) 2289–2292.
- [36] B. D’Urso, O. Painter, J. O’Brien, T. Tombrello, A. Yariv, A. Scherer, Modal reflectivity in finite-depth two-dimensional photonic crystal microcavities, *J. Opt. Soc. Am. B* 15 (1998) 1155–1159.
- [37] O. Painter, J. Vuckovic, A. Scherer, Defect modes of a two-dimensional crystal in an optically thin dielectric slab, *J. Opt. Soc. Am. B* 16 (1999) 275–285.
- [38] S. Fan, P.R. Villeneuve, J.D. Joannopoulos, High extraction efficiency of spontaneous emission from slabs of photonic crystals, *Phys. Rev. Lett.* 78 (1997) 3294.
- [39] M. Boroditsky, T.F. Krauss, R. Coccioli, R. Vrijen, R. Bhat, E. Yablonovitch, Light extraction from optically pumped light-emitting diode by thin-slab photonic crystal, *Appl. Phys. Lett.* 75 (1999) 1036–1038.
- [40] M.R. Krames et al., High-power truncated-inverted-pyramid $(\text{Al}_x\text{Ga}_{1-x})_{0.5}\text{In}_{0.5}\text{P}/\text{GaP}$ light-emitting diodes exhibiting > 50% external quantum efficiency, *Appl. Phys. Lett.* 75 (1999) 2367.
- [41] M. Rattier et al., High extraction efficiency, laterally injected, light emitting diodes combining microcavities and photonic crystals, *Opt. Quantum Electron.*, in press.
- [42] E. Chow et al., Three-dimensional control of light in a two-dimensional crystal slab, *Nature* 407 (2000) 983–986.
- [43] E. Chow, S.Y. Lon, J.R. Wendt, S.G. Johnson, J.D. Joannopoulos, Quantitative analysis of bending efficiency in photonic crystal waveguide bends at $\lambda = 1.55 \mu\text{m}$ wavelengths, *Opt. Lett.* 26 (2001) 286–288.
- [44] T.F. Krauss, R.M. De La Rue, S. Brand, Two-dimensional photonic-bandgap structures operating at near-infrared wavelengths, *Nature* 383 (1996) 699–702.
- [45] D. Labilloy et al., in: H. Benisty, J.-M. Gérard, R. Houdré, J. Rarity, C. Weisbuch (Eds.), *Fundamentals and Applications of Confined Photon Systems*, Springer, Heidelberg, 1999.
- [46] D. Labilloy, H. Benisty, C. Weisbuch, C.J.M. Smith, T.F. Krauss, R. Houdré, U. Oesterle, Finely resolved transmission spectra and band structure of two-dimensional photonic crystals using InAs quantum dots emission, *Phys. Rev. B* 59 (1999) 1649–1652.
- [47] D. Labilloy et al., Quantitative measurement of transmission, reflection and diffraction of two-dimensional photonic bandgap structures at near-infrared wavelengths, *Phys. Rev. Lett.* 79 (1997) 4147–4150.

- [48] D. Labilloy, H. Benisty, C. Weisbuch, T.F. Krauss, R. Houdré, U. Oesterle, Use of guided spontaneous emission of a semiconductor to probe the optical properties of two-dimensional photonic crystals, *Appl. Phys. Lett.* 71 (1997) 738–740.
- [49] See the Optimist web site of the IST-EU program, <http://www.intec.rug.ac.be/ist-optimist/wshp.asp>.
- [50] H. Benisty, D. Labilloy, C. Weisbuch, C.J.M. Smith, T.F. Krauss, A. Béraud, D. Cassagne, C. Jouanin, Radiation losses of waveguide-based two-dimensional photonic crystals: positive role of the substrate, *Appl. Phys. Lett.* 76 (2000) 532–534.
- [51] P. Lalanne, H. Benisty, Ultimate limits of two-dimensional photonic crystals etched through waveguides: an electromagnetic analysis, *J. Appl. Phys.* 89 (2001) 1512–1514.
- [52] H. Benisty, P. Lalanne, S. Olivier, M. Rattier, C. Weisbuch, C.J.M. Smith, T.F. Krauss, C. Jouanin, D. Cassagne, Finite-depth and intrinsic losses in vertically etched two-dimensional photonic crystals, *Opt. Quantum Electron.*, in press.
- [53] W. Bogaerts et al., Out-of-plane scattering in photonic crystals, *IEEE Phot. Technol. Lett.* 13 (2001) 565–567.
- [54] D. Labilloy, H. Benisty, C. Weisbuch, T.F. Krauss, C.J.M. Smith, R. Houdré, U. Oesterle, High-finesse disk microcavity based on a circular Bragg reflector, *Appl. Phys. Lett.* 73 (1998) 1314–1316.
- [55] C. Grillet et al., Characterisation of 2D photonic crystals cavities on InP membranes, *Eur. Phys. J. D*, in press; X. Letartre, C. Seassal, C. Grillet, Group velocity and propagation losses measurement in a single-line photonic-crystal waveguide on InP membranes, *Appl. Phys. Lett.* 79 (2001) 2312.
- [56] C.J.M. Smith, R.M. De La Rue, M. Rattier, S. Olivier, H. Benisty, C. Weisbuch, T.F. Krauss, R. Houdré, U. Oesterle, Coupled guide and cavity in a two-dimensional photonic crystal, *Appl. Phys. Lett.* 78 (2001) 1487–1489.
- [57] S. Olivier, H. Benisty, M. Rattier, C. Weisbuch, M. Qiu, A. Karlsson, C.J.M. Smith, R. Houdré, U. Oesterle, Resonant and nonresonant transmission through waveguide bends in a planar photonic crystal, *Appl. Phys. Lett.* 79 (2001) 2514–2516.
- [58] A. Talneau, L. Le Gouezigou, N. Bouadma, Quantitative measurements of low propagation losses at 1.55 μm on planar photonic crystal waveguides, *Opt. Lett.* 26 (2001) 1259–1261.
- [59] J. Moosbürger, M. Kamp, A. Forchel, Paper JTUB2, Transmission spectra measurements on photonic crystals based bent waveguides, in: CLEO, Baltimore, May 6–11, 2001.
- [60] S.Y. Lin, E. Chow, S.G. Johnson, J.D. Joannopoulos, Demonstration of highly efficient waveguiding in a photonic crystal slab at the 1.5 μm wavelength, *Opt. Lett.* 25 (2000) 1297–1299.
- [61] S. Noda, A. Chutinan, M. Imada, Trapping and emission of photons by a single defect in a photonic bandgap structure, *Nature* 407 (2000) 608–610.
- [62] L. Raffaele, R.M. De La Rue, J.S. Roberts, T.F. Krauss, Edge-emitting semiconductor microlasers with ultrashort-cavity and dry-etched high-reflectivity photonic microstructure mirrors, *IEEE Photon. Technol. Lett.* 13 (2001) 176–178.
- [63] O.J. Painter, A. Husain, A. Scherer, J.D. O'Brien, I. Kim, Dapkus, Room temperature photonic crystal defect lasers at near-infrared wavelengths in InGaAsP, *J. Lightwave Technol.* 17 (1999) 2082–2088.
- [64] H.-G. Park, J.-K. Hwang, J. Huh, H.-Y. Ryu, Y.-H. Lee, J.-S. Kim, Nondegenerate monopole-mode two-dimensional photonic band gap laser, *Appl. Phys. Lett.* 79 (2001) 3032–3034.
- [65] H. Rigneault, F. Lemarchand, A. Sentenac, Dipole radiation into grating structures, *J. Opt. Soc. Am. A* 17 (2000) 1048–1058.
- [66] M. Forchel et al., Lasers with PBG mirrors, in: IPRM'99, Davos, 1999.
- [67] T.D. Happ, M. Kamp, F. Klopff, J.P. Reithmaier, A. Forchel, Bent laser cavity based on 2D photonic crystal waveguide, *Electron. Lett.* 26 (2000) 324–325.
- [68] R. März, in: B. Culshaw, A. Rogers, A. Taylor (Eds.), *Integrated Optics: Design and Modeling*, The Artech House Optoelectronics Library, Artech House, Boston, 1994.
- [69] A. Ortigosa-Blanch, J.C. Knight, W.J. Wadsworth, J. Arriaga, B.J. Mangan, T.A. Birks, P.St.J. Russel, Highly birefringent photonic crystal fibres, *Opt. Lett.* 25 (2000) 1325–1327.